

SEPTEMBER 2014

M.Sc. Thesis in Engineering of Physics

MEHMET ARSLAN

**UNIVERSITY OF GAZIANTEP
GRADUATE SCHOOL OF
NATURAL & APPLIED SCIENCES**

**RECONSTRUCTION OF NEUTRAL PIONS
FROM PHOTON CONVERSIONS**

**M. Sc. THESIS
IN
ENGINEERING OF PHYSICS**

**BY
MEHMET ARSLAN
SEPTEMBER 2014**

Reconstruction of Neutral Pions
From Photon Conversions

M.Sc. Thesis

in

Engineering Physics

University of Gaziantep

Supervisor

Prof. Dr. Ayda BEDDALL

by

Mehmet ARSLAN

September 2014

© 2014 [Mehmet ARSLAN]

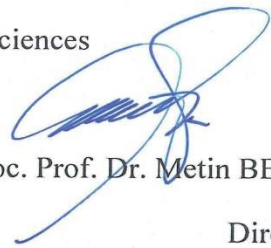
REPUBLIC OF TURKEY
UNIVERSITY OF GAZIANTEP
GRADUATE SCHOOL OF NATURAL & APPLIED SCIENCES
ENGINEERING PHYSICS

Name of the thesis: Reconstruction of Neutral Pions from Photon Conversions

Name of the student: Mehmet ARSLAN

Exam date: 03.09.2014

Approval of the Graduate School of Natural and Applied Sciences


Assoc. Prof. Dr. Metin BEDİR


Director

I certify that this thesis satisfies all the requirements as a thesis for the degree of Master of Science


Prof. Dr. A. Necmeddin YAZICI

Head of Department

This is to certify that we have read this thesis and that in our ~~consensus~~/majority opinion it is fully adequate, in scope and quality, as a thesis for the degree of Master of Science.


Prof. Dr. Ayda BEDDALL

Supervisor




Examining Committee Members

Prof. Dr. Ayda BEDDALL

Assoc. Prof. Dr. Ahmet BİNGÜL

Assist. Prof. Dr. Andrew BEDDALL

Signature

I hereby declare that all information in this document has been obtained and presented in accordance with academic rules and ethical conduct. I also declare that, as required by these rules and conduct, I have fully cited and referenced all material and results that are not original to this work.

Mehmet ARSLAN

ABSTRACT

RECONSTRUCTION OF NEUTRAL PIONS FROM PHOTON CONVERSIONS

ARSLAN, Mehmet

M.Sc. in Physics Eng.

Supervisor: Prof. Dr. Ayda BEDDALL

September 2014

28 page

In this study, the low energetic photon conversion process in the ATLAS detector has been discussed. The conversion candidates selected from minimum bias events at $\sqrt{s} = 8$ TeV are used to reconstruct π^0 particles built from two-photon invariant mass distribution. A clear π^0 peak is obtained and fitted to Gaussian function. The results reveal that purity of the π^0 signal depends strongly on the χ^2 value of the e^+e^- pairs. It is also found that the optimal mass window cut for selecting π^0 candidates is around $\pm 2\sigma$ around the π^0 peak.

Key Words: photon conversion, ATLAS, reconstruction of π^0 .

ÖZET

FOTON DÖNÜŞÜMLERİNDEN YÜKSÜZ PİYONLARIN ELDE EDİLMESİ

ARSLAN, Mehmet
Yüksek Lisans Tezi, Fizik Müh. Bölümü
Tez Yöneticisi: Prof. Dr. Ayda BEDDALL
Eylül 2014
28 sayfa

Bu çalışmada, ATLAS dedektöründeki düşük enerjili foton dönüşüm süreçleri tartışıldı. 8 TeV minimum meyil verilerinden seçilen foton dönüşüm adayları iki foton değişmez kütle dağılımından π^0 parçacıklarını oluşturmak için kullanıldı. Temiz π^0 tepe noktası elde edildi ve Gauss fonksiyonuna uyduruldu. Sonuçlar π^0 sinyalinin saflığının kuvvetli bir şekilde e^+e^- çiftlerinin χ^2 değerine bağlı olduğunu ve π^0 adaylarını seçmek için en uygun kütle seçim penceresinin π^0 tepe noktasının $\pm 2\sigma$ etrafında olduğunu ortaya çıkarmıştır.

Anahtar Kelimeler: foton dönüşümü, ATLAS, π^0 elde edilmesi.

To my family

ACKNOWLEDGEMENTS

Foremost, I would like to express my sincere gratitude to my supervisor Prof. Dr. Ayda BEDDALL and to my advisors Assoc. Prof. Dr. Ahmet BİNGÜL and Asist. Prof. Dr. Andrew BEDDALL for the continuous support of my M. Sc. Study and research, for their patience, motivation, enthusiasm and immense knowledge. Their guidance helped me in all the time of research and writing of this thesis. I could not have imagined having a better advisor and mentor M. Sc. study.

Meanwhile, I want to say thank to my research colleagues in the department for their friendship and pleasant coffee break conservations.

Finally, I would like to thank to my parents Burhan and Meryem ARSLAN, my brothers, my grandparents and also my darling Yağmur KAR for their spiritual supports and patients.

TABLE OF CONTENTS

	PAGE
ABSTRACT	v
ÖZET	vi
ACKNOWLEDGEMENTS	viii
TABLE OF CONTENTS	ix
LIST OF TABLES	x
LIST OF FIGURES	xi
LIST OF SYMBOLS/ABBREVIATIONS	xii
CHAPTER 1: INTRODUCTION	1
CHAPTER 2: THE LHC AND THE ATLAS DETECTOR	2
2.1 The Large Hadron Collider (LHC)	2
2.2 The ATLAS Detector	2
CHAPTER 3: RECONSTRUCTION OF NEUTRAL PIONS FROM PHOTON CONVERSIONS	3
3.1 A Photon Conversion	4
3.1.1. Cross Section	5
3.2. Photon Conversions and π^0 Reconstruction in ATLAS	9
CHAPTER 4: CONCLUSION	24
REFERENCES	25
APPENDIX A: π^0 FORMULAE	26
A.1 Two-Photon Invariant Mass Formula	26
A.2 π^0 Mass Resolution Formula	27

LIST OF TABLES

	PAGE
Table 3.1: Number of generated photons and photon conversions in ATLAS. 20% of photons converted into $e + e -$ pairs but 9,122,610 photon conversions cannot detect in the ATLAS detector.....	10
Table 3.2: The applied cuts to photon conversions for reconstruction of neutral pions.....	15
Table 3.3: Detailed statistical results for Figure 3.22.	22

LIST OF FIGURES

	PAGE
Figure 3.1. (a) Probability for a photon to have converted as a function of radius for different values of $ \eta $, shown for photons with $p_T > 1$ GeV in minimum-bias events [6]. (b) The photon conversion and the tracks of the electron-positron pair in the ATLAS inner detector.....	3
Figure 3.2. Schematic diagram of a photon conversion.....	4
Figure 3.3. Material distribution in ATLAS as a function of pseudorapidity [2].	6
Figure 3.4. The graph of the probability density function for electron.	7
Figure 3.5. ΔR vs ΔE distribution for matching. All candidates below the yellow line can be assumed to be a signal.....	11
Figure 3.6. The χ^2 distributions for conversion signals and backgrounds.	11
Figure 3.7. Conversion radius distributions of the signal and background.....	12
Figure 3.8. Conversion points of the signal and background in x-y plane.....	12
Figure 3.9. Production points of conversions in the range -1200 to 1200 mm.	13
Figure 3.10. Inner part of the ID in the range -150 to 150 mm. Three layers of the pixel detector, the cooling pipe of layers and the beampipe are seen clearly.	13
Figure 3.11. Invariant mass distributions of the signal and background.	14
Figure 3.12. Two photon invariant mass distribution for $\chi^2 \leq 1$	16
Figure 3.13. Two photon invariant mass distribution for $\chi^2 \leq 2$	16
Figure 3.14. Two photon invariant mass distribution for $\chi^2 \leq 3$	17
Figure 3.15. Two photon invariant mass distribution for $\chi^2 \leq 4$	17
Figure 3.16. Two photon invariant mass distribution for $\chi^2 \leq 5$	18
Figure 3.17. Two photon invariant mass distribution for $\chi^2 \leq 6$	18
Figure 3.18. Two photon invariant mass distribution for $\chi^2 \leq 7$	19
Figure 3.19. Two photon invariant mass distribution for $\chi^2 \leq 8$	19
Figure 3.20. Two photon invariant mass distribution for $\chi^2 \leq 9$	20
Figure 3.21. Two photon invariant mass distribution for $\chi^2 \leq 10$	20
Figure 3.22. Purity, Efficiency and Purity \times Efficiency plots as a function of mass width (σ) for different χ^2 values.....	21

LIST OF SYMBOLS/ABBREVIATIONS

p : Proton

A : Heavy ion; atomic mass

e^- : Electron

e^+ : Positron

π^0 : Neutral pi-meson

p_T : Transverse momentum

σ : Resolution (momentum, energy, mass or spatial); cross-section

\oplus : Quadratic sum

ϕ : Azimuthal angle

θ : Polar angle

η : Pseudorapidity; eta meson

R : Radial extension

\vec{P} : Particle space momentum vector

γ : Photon

m : Particle mass; invariant mass

E : Particle energy

X_0 : Radiation length

N_A : Avogadro's number

Z : Atomic number

P : Probability density function; purity

λ : Mean free path

χ^2 : Chi-square value

K_S^0 : Neutral short-lived K meson

r : Conversion radius

θ_{12} : Opening angle between photon 1 and 2

ε : Efficiency

CHAPTER 1

INTRODUCTION

The Large Hadron Collider (LHC) at CERN is the largest and most powerful particle accelerator in the world [1]. The ATLAS (A Toroidal LHC ApparatuS) [2] is a general purpose detector which has been built for observation proton-proton (p-p) and heavy ion-heavy ion (A-A) collisions. High energy proton-proton collisions at LHC can produce in events that contain high multiplicity of hadronic and leptonic particles. In addition, there are many photons in the list of final state particles in ATLAS detector. High-energy photons pass through the ATLAS Inner Detector and deposit their energy in the ATLAS Calorimeter. The low-energy photons convert into electron-positron (e^+e^-) pairs in the ATLAS Inner detector and conversions are recognized from their secondary vertices.

In this study, photon conversions are reconstructed in the inner detector (the Pixel detector, SCT detector, and TRT detector) and neutral pion (π^0) candidates are also reconstructed from conversions. Some cuts are developed to optimally select conversions, and the neutral pion signals are observed by maximizing purity \times efficiency.

Chapter 2 describes general information about the experimental apparatus; the LHC [3] and the ATLAS detector. In Chapter 3, by using ATLAS full simulation and real data [4, 5], the optimal selection of the photon conversion candidates that contain both signals and backgrounds are given. And also how to extract the neutral pion signals from these conversion candidates are given. Finally, a conclusion of the thesis is given in Chapter 4.

CHAPTER 2

THE LHC AND THE ATLAS DETECTOR

2.1 The Large Hadron Collider (LHC)

The Large Hadron Collider (LHC) [3] at CERN is 27 km ring which provide 14 TeV proton-proton collisions at design luminosity of $10^{34} \text{ cm}^{-2}\text{s}^{-1}$. Inside the LHC, 2808 bunches of up to 10^{11} protons are collide 40 million times per second. Heavy ions are also collide inside the LHC ring, in particular lead nuclei, a center of mass energy of 5.5 TeV per nucleon pair, at a design luminosity of $10^{27} \text{ cm}^{-2}\text{s}^{-1}$.

2.2 The ATLAS Detector

The ATLAS (A Toroidal LHC ApparatuS) [2] is a general purpose detector which have been built for observation p-p and A-A collisions. The ATLAS is 44m in length, 25m in height, and the weight of the detector is approximately 7000 tones.

Presented here is a summary of the main features of the apparatus, more detailed accounts can be found elsewhere [2, 3].

CHAPTER 3

RECONSTRUCTION OF NEUTRAL PIONS FROM PHOTON CONVERSIONS

In proton-proton collision at LHC many photons occur as a final state particle in the ATLAS detector. The high energetic photons pass through the ATLAS Inner detector and deposit their energies in the ATLAS Calorimeter. Overall about 50 % of photons are converted into an electron-positron (e^+e^-) pair before reaching calorimeter as illustrated in Figure 3.1 (a), and the Figure 3.1 (b) shows us the photon conversion and tracks of the electron-positron pair in the ATLAS inner detector.

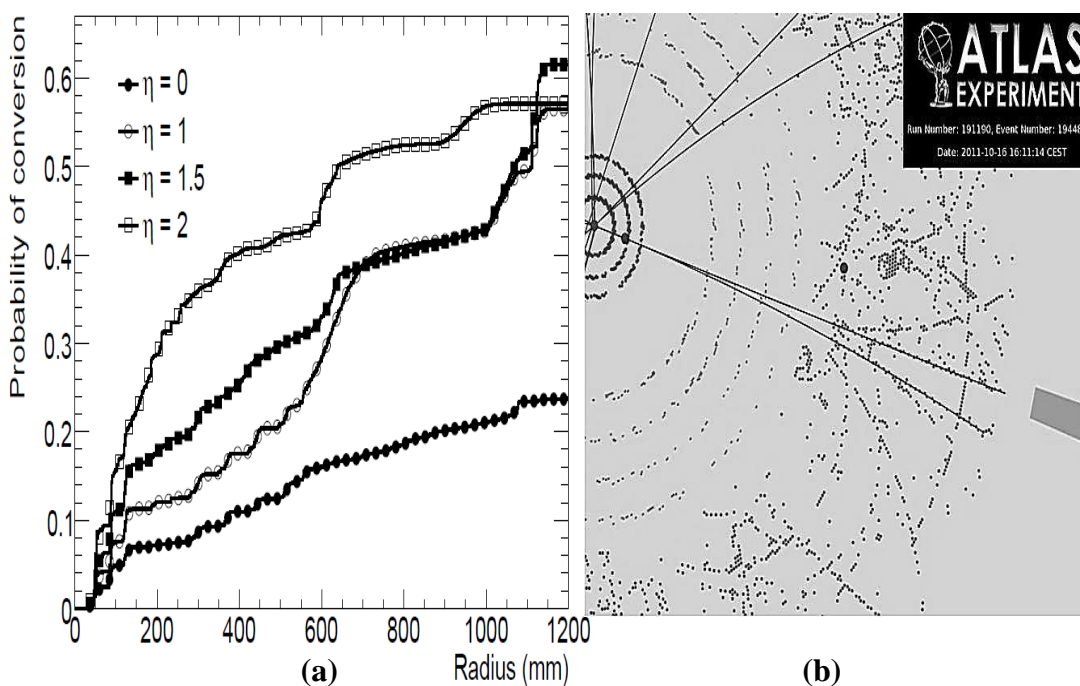


Figure 3.1. (a) Probability for a photon to have converted as a function of radius for different values of $|\eta|$, shown for photons with $p_T > 1$ GeV in minimum-bias events. The probability is not a strong function of the photon energy [6]. (b) The photon conversion and the tracks of the electron-positron pair in the ATLAS inner detector.

In this study, low p_T photons are reconstructed from electron-positron pairs and neutral pions are reconstructed from photon conversions in minimum-bias events.

3.1 A Photon Conversion

When a photon passes near a heavy nucleus, it disintegrates and produces electron-positron ($e^+ e^-$) pairs, which is called a photon conversion. Electron and positron always move in different directions so that the momentum is conserved, Figure 3.2.

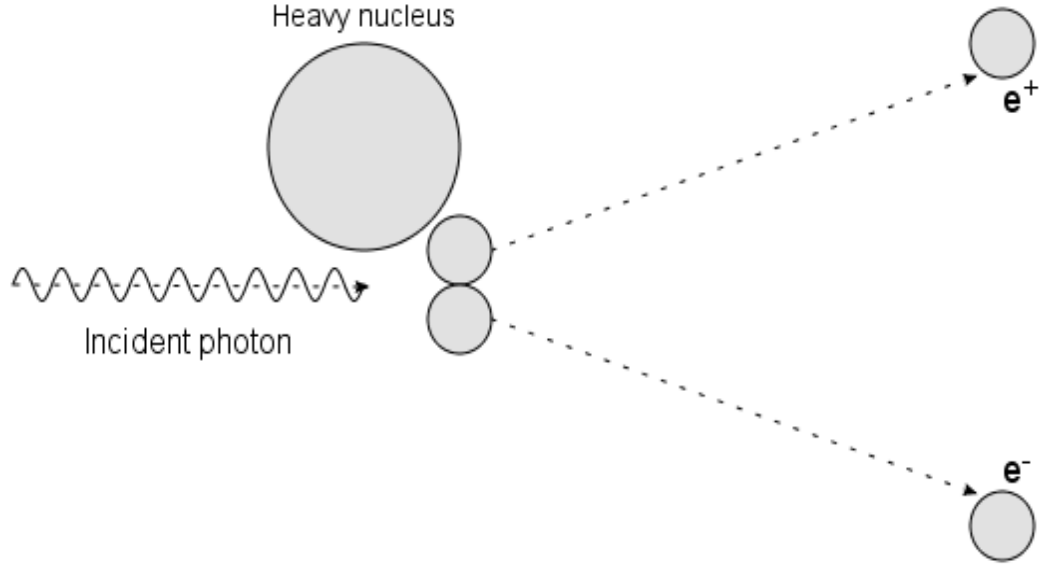


Figure 3.2. Schematic diagram of a photon conversion.

Since the momentum and energy cannot be conserved simultaneously, a photon conversion does not occur in vacuum (free space). Minimum required energy for this process is described below mathematically.

Conservation of momentum:

$$P_\gamma = P_N \text{ or } E_\gamma = P_N \quad (3.1)$$

where P_γ is the momentum of incident photon, P_N is the momentum of a heavy nucleus, and E_γ is the energy of incident photon.

Conservation of energy:

$$E_\gamma + m_N c^2 = \sqrt{m_N^2 c^4 + P_N^2 c^2} + 2m_e c^2 \quad (3.2)$$

where m_N is the mass of a heavy nucleus, $m_e = 0.511 \text{ MeV}/c^2$ is the mass of electron.

Substituting from the equation (3.1):

$$E_\gamma + m_N c^2 = \sqrt{m_N^2 c^4 + E_\gamma^2} + 2m_e c^2 \quad (3.3)$$

Then, we can solve the equation (3.3) for E_γ :

$$E_\gamma = \frac{2m_e(1 - m_e/m_N)}{(1 - 2m_e/m_N)} \quad (3.4)$$

Here, $m_N \gg m_e$, so $\frac{m_e}{m_N} \cong 0$:

$$E_\gamma = 2m_e \quad (3.5)$$

Finally, we found that the minimum incident photon energy required to produce e^+e^- pair is:

$$E_\gamma = 1.022 \text{ MeV}/c^2 \quad (3.6)$$

3.1.1. Cross Section

For photon energies of 1 GeV and above the cross section for the conversion process [6] is almost completely independent of the energy of the incident photon, and may be given by the following equation:

$$\sigma = \frac{7A}{9X_0N_A} \quad (3.7)$$

where A is the atomic mass of target, and $N_A = 6.022 \times 10^{23}$ is Avogadro's number, X_0 is the radiation length* of the material through which the photon passes, and the radiation length is calculated approximately by the following analytical formula [7]:

$$X_0 = \frac{716.4 A}{Z(Z + 1) \ln\left(\frac{287}{\sqrt{Z}}\right)} \text{ g cm}^{-2} \quad (3.8)$$

The amount of material in the ATLAS Inner Detector given in the radiation length and the interaction length as a function of pseudorapidity, can be seen in Figure 3.3.

* This radiation length is defined such that it is 7/9 of the mean free path for photon conversion.

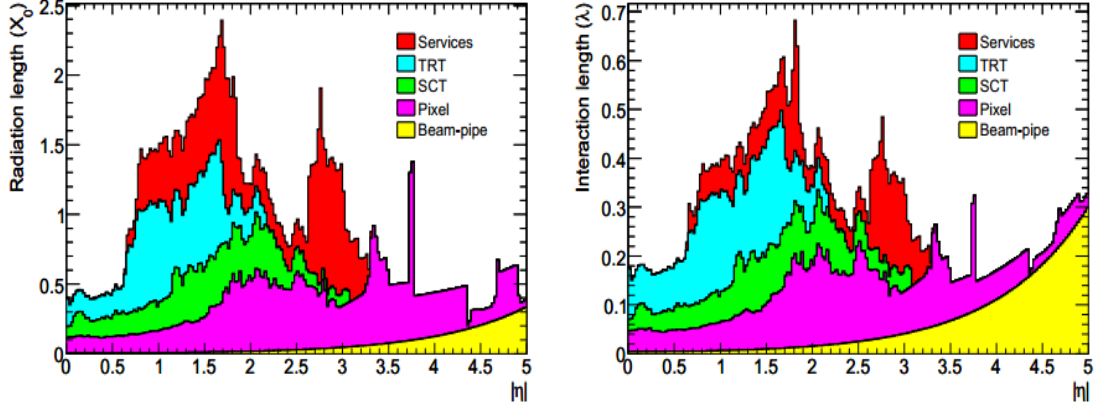


Figure 3.3. Material distribution in ATLAS as a function of pseudorapidity [2].

The differential cross section for photon conversions of energies of 1 GeV and above in terms of the quantity $x = (E_{electron}/E_{photon})$ is:

$$\frac{d\sigma}{dx} = \frac{A}{X_0 N_A} \left(1 - \frac{4}{3}x(1-x)\right) \quad (3.9)$$

This cross section is symmetric in x and $1-x$, the electron and positron energies, it implies that the momentum of the photon is not simply shared equally between the electron and the positron.

The probability density function for the energy of electron (or positron) can be found as follows. One can define a function:

$$f(x) = \frac{d\sigma}{dx} = \frac{A}{X_0 N_A} \left(1 - \frac{4}{3}x(1-x)\right), x \in (0, 1) \quad (3.10)$$

Integral of $f(x)$ yields:

$$\int_0^1 f(x) dx = \int_0^1 \frac{A}{X_0 N_A} \left(1 - \frac{4}{3}x(1-x)\right) dx = \frac{7A}{9X_0 N_A} \quad (3.11)$$

Finally, the probability density function $P(x)$ is defined as:

$$P(x) = \frac{f(x)}{\int_0^1 f(x) dx} \quad (3.12)$$

Substituting (3.10) and (3.11) into (3.12) result in:

$$P(x) = \frac{9}{7} \left(1 - \frac{4}{3}x(1-x) \right) \quad (3.13)$$

So that:

$$\int_0^1 P(x) dx = \int_0^1 \frac{9}{7} \left(1 - \frac{4}{3}x(1-x) \right) dx = 1 \quad (3.14)$$

The graph of the equation (3.13), x takes on a value in the interval $[0, 1]$, are shown in Figure 3.4.

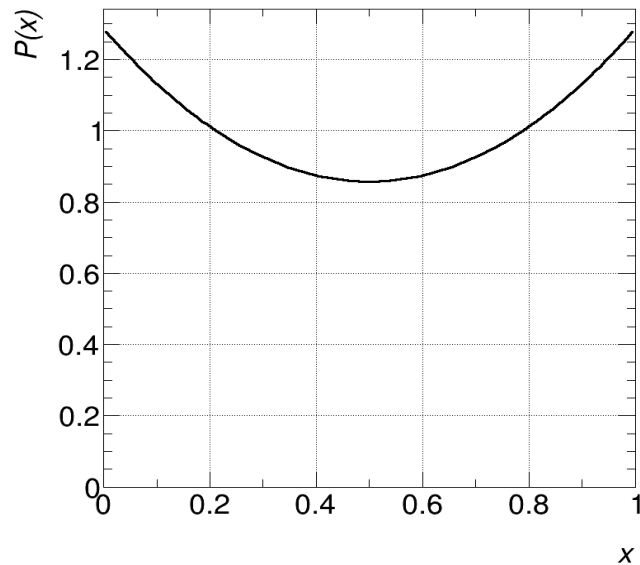


Figure 3.4. The graph of the probability density function for electron.

The graph is same for an electron and positron because of the cross-section is symmetric in x and $1 - x$. This graph shows us either the electron or the positron may be produced with a very low energy.

This is the simple way to calculate the cross-section of photon conversion. However, there is a more sophisticated method for a computation of cross-section. The ATLAS detector simulation program, GEANT4 (GEometry ANd Tracking) [4] uses the following method for calculating the total cross-section.

In the GEANT4, the total cross-section [8] per atom for the photon conversion into an (e^+e^-) pair has been parameterized as

$$\sigma(Z, E_\gamma) = Z(Z + 1) \left[F_1(X) + F_2(X) Z + \frac{F_3(X)}{Z} \right], \quad (3.15)$$

where E_γ is the incident photon energy and $X = \ln(E_\gamma/m_e c^2)$. The functions F_n are given by

$$F_1(X) = a_0 + a_1 X + a_2 X^2 + a_3 X^3 + a_4 X^4 + a_5 X^5 \quad (3.16)$$

$$F_2(X) = b_0 + b_1 X + b_2 X^2 + b_3 X^3 + b_4 X^4 + b_5 X^5$$

$$F_3(X) = c_0 + c_1 X + c_2 X^2 + c_3 X^3 + c_4 X^4 + c_5 X^5$$

with the parameters a_i , b_i , c_i taken from a least-squares fit to the data [9]. Their values can be found in the function which computes the formula (3.15). This parameterization describes the data in the range $1 \leq Z \leq 100$ and $E_\gamma \in [1.5 \text{ MeV}, 100 \text{ GeV}]$.

The accuracy of the fit was estimated to be $\frac{\Delta\sigma}{\sigma} \leq 5\%$ with a mean value of $\approx 22\%$. Above 100 GeV the cross section is constant. Below $E_{low} = 1.5 \text{ MeV}$ the extrapolation

$$\sigma(E) = \sigma(E_{low}) \left(\frac{E - 2m_e c^2}{E_{low} - 2m_e c^2} \right)^2 \quad (3.17)$$

is used.

In a given material the mean free path, λ , for a photon to convert into an (e^+e^-) pair is

$$\lambda(E_\gamma) = \left(\sum_i n_{ati} \sigma(Z_i E_\gamma) \right)^{-1} \quad (3.18)$$

where n_{ati} is the number of atoms per volume of the i^{th} element of the material.

3.2. Photon Conversions and π^0 Reconstruction in ATLAS

In the ATLAS detector, the reconstruction of photon conversions is important to understand different physics measurements which involve electromagnetic decay product. In addition, photons are the final state product of many particles such as a neutral pion (π^0), eta (η^0), e.t.c., and Higgs boson. Also we can use conversion vertices for mapping a localization of material in the ATLAS tracker. Actually, the ATLAS detector cannot detect photons directly. We can only observe photons after they interact with matter and also deposit their energies in the calorimeter of the ATLAS system.

In this study, the photon conversion process is used for detecting photons. Many photon convert into (e^+e^-) pairs in the ATLAS tracker, and these conversions are recognized from secondary vertices containing two tracks. Some parameters of these tracks are recorded by the detector such as q/p , χ^2 (which comes from track and vertex fitting algorithm), η , ϕ and the production point of conversion in x-y-z direction. But, some decays are similar to the photon conversion, for example neutral short-lived kaon (K_S^0) decay into two opposite charged pion, these decays are also recorded to the ATLAS conversion data, so the ATLAS data contains conversion candidates that contain both conversions (signal) and background. Therefore, it is required to develop some cuts for optimal selection of photon conversions.

The ATLAS full Monte Carlo (MC) simulation can be used to optimize cuts for selection of true conversions. This MC data contains both generator level and reconstructed level events. In the generator level we know all particles and decays because the particle generator program produce particles and decays and saves these events into the data files in this level. Reconstructed level is the event simulation of the ATLAS detector for these events. By matching truth and reconstructed events, one can find the true photon conversions to define signal properties and optimal selection cuts. The results from MC studies can be used in real data to select the real photon conversions.

The MC data includes about one million minimum bias events, with $\sqrt{s} = 8$ TeV. The data files have four containers, which are Tracks, CaloClusters, Conversions, MonteCarlos. Each container contains four-vectors and associated properties for the particles.

Note that some fraction of photon conversions will be highly asymmetric, and either the electron or the positron may be produced with a very low energy. If this energy falls below the threshold required to produce a reconstructable track in ATLAS tracker, then the converted photon will be seen to have only one track called single conversion and will be difficult to distinguish from a single electron or positron.

Table 3.1 shows number of generated photons versus single or double converted photons and number of photons reached to calorimeter. In this study we will only consider double conversions.

Table 3.1: Number of generated photons and photon conversions in ATLAS. 20% of photons converted into e^+e^- pairs but 9,122,610 photon conversions cannot detect in the ATLAS detector.

Number of generated photons	Number of double conversion	Number of single conversion	Number of photons in ECAL
60,769,508	278,655	2,859,665	48,508,578

For matching truth and reconstructed conversions, azimuthal angle (ϕ), pseudorapidity (η) and energy (E) parameters are used. Photons are collected from electron-positron pairs in the reconstructed level. Then, these reconstructed level photons are matched to the generator level conversions by using ΔR (pseudorapidity-azimuthal angle space) values and ΔE (energy difference) values. ΔR is defined as $\Delta R = \sqrt{\Delta\eta^2 + \Delta\phi^2}$. Here $\Delta\eta$ is the pseudorapidity (η) differences between the reconstructed level and the generator level photons, and $\Delta\phi$ is the azimuthal angle (ϕ) differences between the reconstructed level and the generator level photons. The energy difference (ΔE) is defined as $\Delta E = |E_{rec} - E_{gen}|/E_{gen}$. A plot of ΔR vs ΔE is shown in Figure 3.5 for the signal candidates. Signal tends to have small ΔR and ΔE values. The yellow line is used for discriminating signals from backgrounds. If ΔR and ΔE values of a reconstructed particle is below this line one can assume that it is a signal and background otherwise. After selecting signal candidates, it is straight forward to investigate signal and background properties.

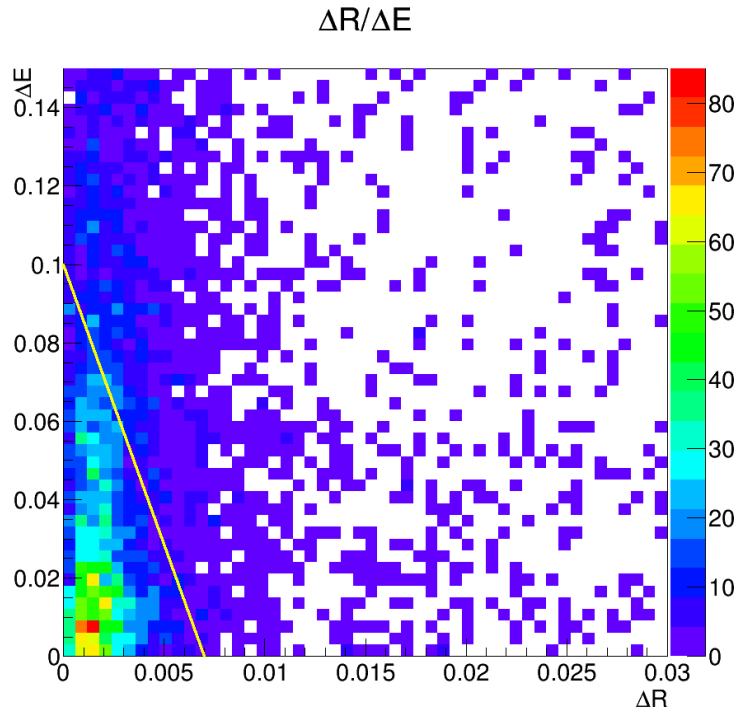


Figure 3.5. ΔR vs ΔE distribution for matching. All candidates below the yellow line can be assumed to be a signal.

Figure 3.6 shows the χ^2 distribution of signals and backgrounds. Again signals tend to have lower χ^2 values while backgrounds extend up to relatively larger values. Basically a cut can be applied to discriminate signals from backgrounds.

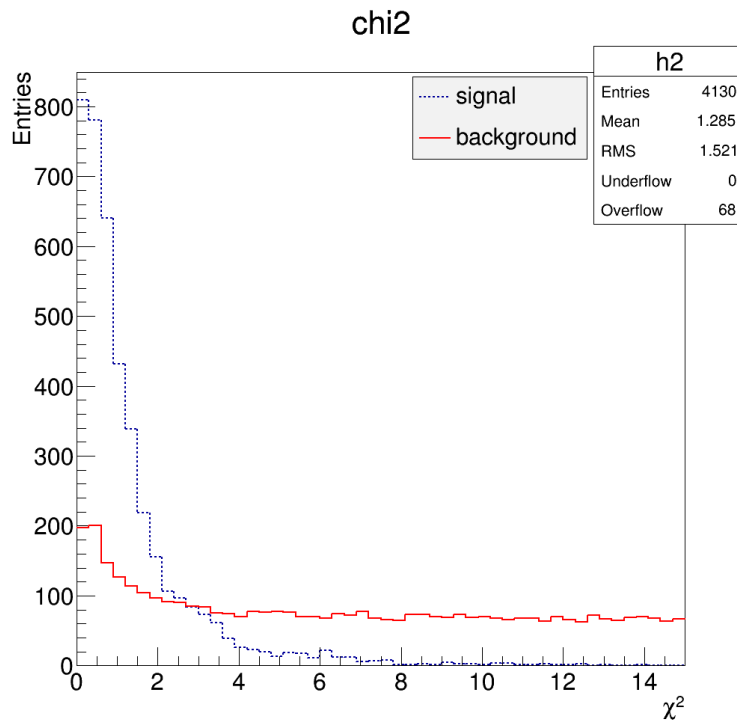


Figure 3.6. The χ^2 distributions for conversion signals and backgrounds.

We may look at conversion radius defined as $r = \sqrt{x^2 + y^2}$, for finding the difference between the signals and backgrounds. But the distributions are nearly the same for signal and background, as shown in Figure 3.7. Many candidates decay into oppositely charged pairs in the detector modules. Only we can eliminate the conversion candidates inside the beampipe, because photon conversions occur when photons interact with the matter*. In addition, the graphs of 2-dimensional (x-y directions) conversion points of signal and background are shown in Figure 3.8.

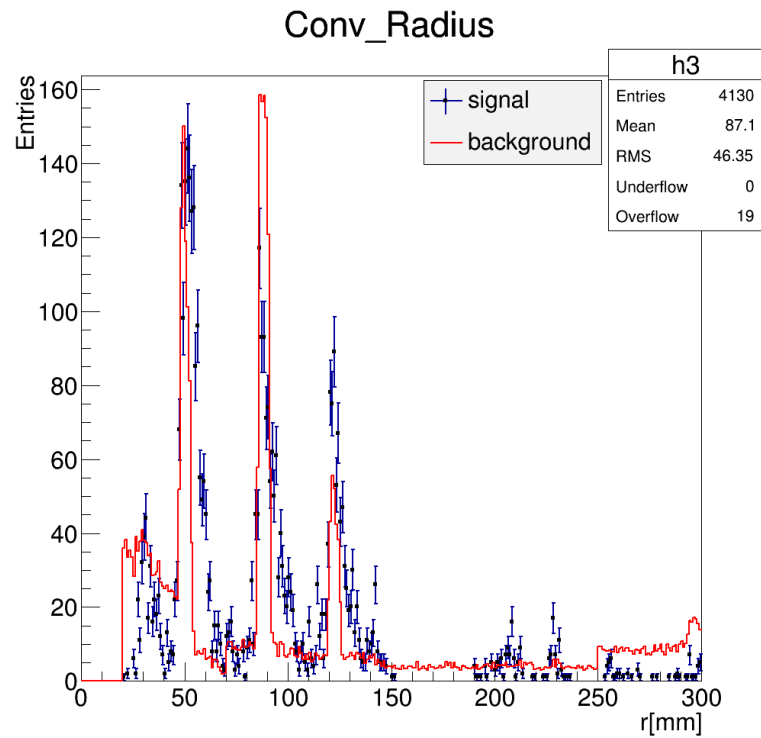


Figure 3.7. Conversion radius distributions of the signal and background.

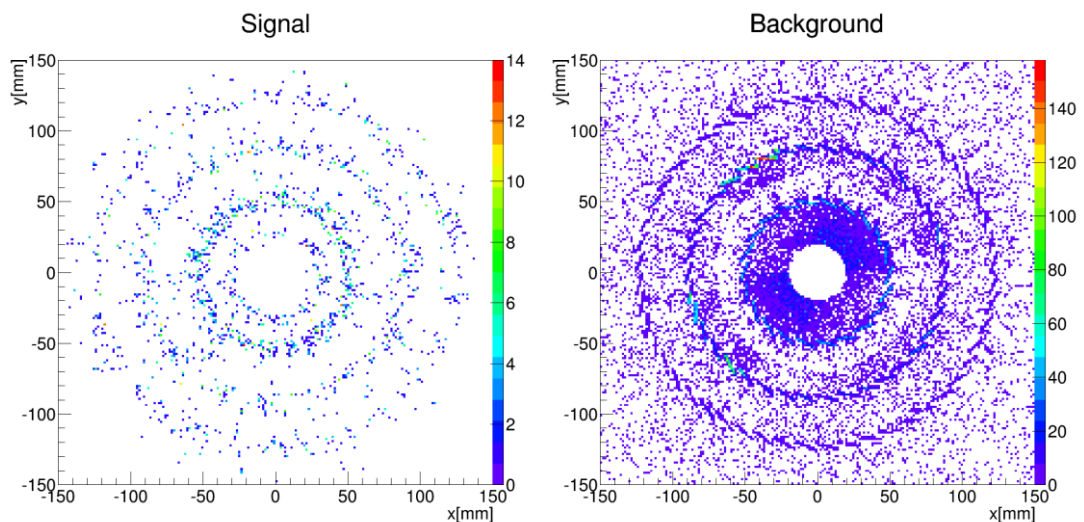


Figure 3.8. Conversion points of the signal and background in x-y plane.

* The inside of the beampipe is a vacuum, so photon conversions cannot occur in the vacuum because of the conservation of momentum.

Figure 3.9 shows production points of photon conversions in ATLAS detector. The parts of the Inner detector are seen very clearly. This can be used for the localization of inner detector parts. Figure 3.10 shows us the inner part of the Inner detector in detail.

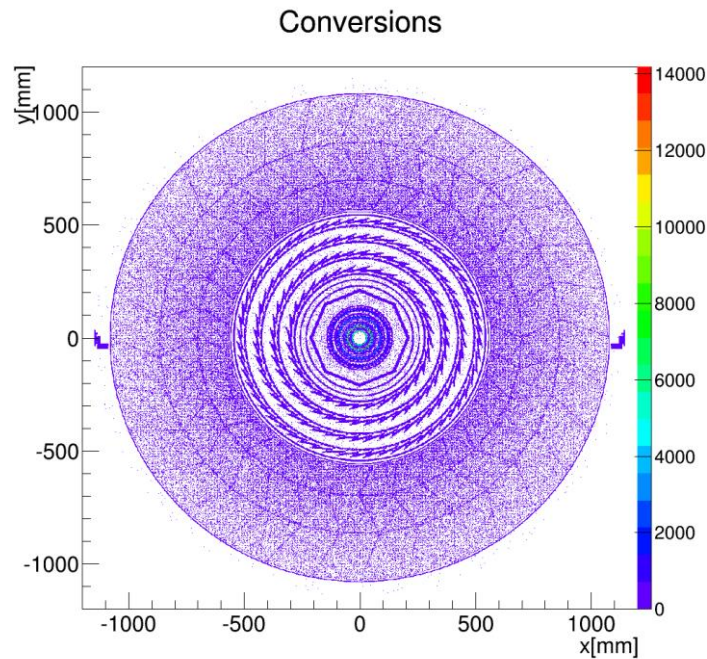


Figure 3.9. Production points of conversions in the range -1200 to 1200 mm.

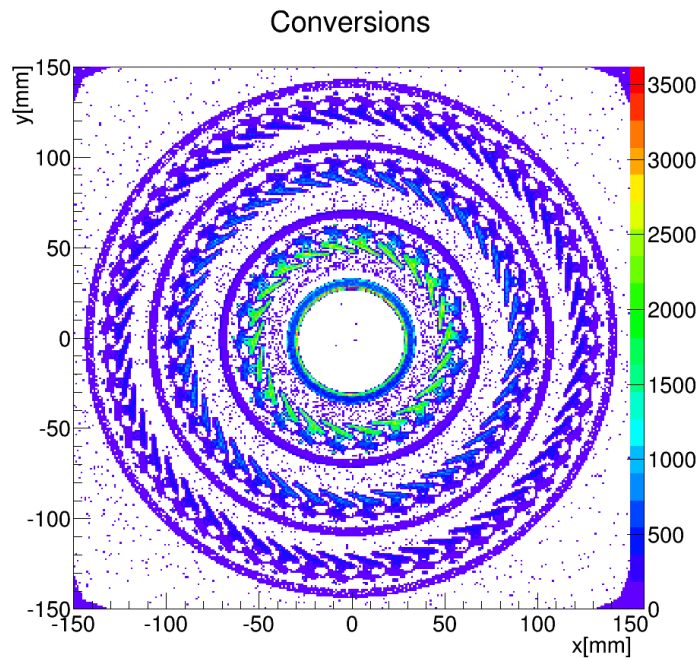


Figure 3.10. Inner part of the ID in the range -150 to 150 mm. Three layers of the pixel detector, the cooling pipe of layers and the beampipe are seen clearly.

Another discrimination parameter is the invariant mass of the conversion candidates. The invariant mass, $m(e^+, e^-)$, of the photon is calculated from:

$$\begin{aligned}
 m^2(e^+, e^-) &= E_\gamma^2 - P_\gamma^2 \\
 &= (E_{e^+} + E_{e^-})^2 - (\vec{P}_{e^+} + \vec{P}_{e^-})^2
 \end{aligned}
 \tag{3.19}$$

where $E_e^2 = P_e^2 + m_e^2$ with $m_e = 0.511 \text{ MeV}/c^2$ for the electron and positron, \vec{P}_{e^\pm} are the measured momentum vectors, and E_{e^\pm} are the calculated particle energies. Electron mass is given to the all candidates, when calculating the invariant mass of the converted particles. The Figure 3.11 shows us the invariant mass of signals and backgrounds. The invariant mass of the signals are less than $1.5 \text{ MeV}/c^2$ but the invariant mass distribution of the background is up to $2.5 \text{ MeV}/c^2$. (The tail of the invariant mass distribution of the signal is shorter than the invariant mass distribution of the background). Therefore, this difference can be used for the elimination of the backgrounds.

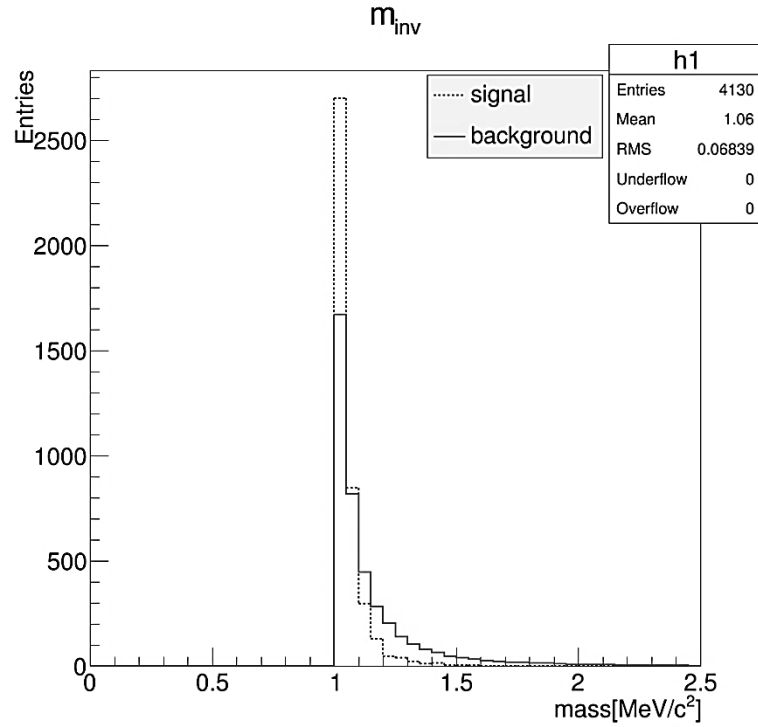


Figure 3.11. Invariant mass distributions of the signal and background.

Neutral pions decay to two photons ($\pi^0 \rightarrow \gamma\gamma$) with a branching ratio of $98.798\% \pm 0.032\%$ [10]. For this analysis, photons are reconstructed from double conversions where both photons are converted in the ATLAS inner detector. The applied cuts to the photon conversions are listed in the Table 3.2.

Table 3.2: The applied cuts to photon conversions for reconstruction of neutral pions.

Parameters	Selected Range
Conversion Radius	$r \geq 30$ mm
Invariant mass	$m \leq 1.5$ MeV/ c^2
Chi2	$\chi^2 \leq 10$
Energy	$E \geq 1000$ MeV
Pseudorapidity	$ \eta \leq 2.5$

Then these photons are used for reconstruction of neutral pions. Invariant mass spectra are formed using the equation*

$$M^2 = 2E_1E_2(1 - \cos \theta_{12}) \quad (3.20)$$

where M is the invariant mass of the reconstructed photons, E_1 and E_2 are energies of photons, and θ_{12} is the angle between two photons [11].

Figure 3.12-21 show the two photon invariant mass distributions, where both photons are converted in the inner detector, as a function of χ^2 values. Clear π^0 signal are observed for lower χ^2 values. While π^0 signal significance is dropping as χ^2 gets larger.

Each distribution is fitted to a Gaussian (for signal) plus a cubic polynomial (for background) functions. Using real data fit results, one can define efficiency and purity [11] as follows.

$$\mathcal{E} = \frac{S}{S_0} \quad (3.21)$$

$$P = \frac{S}{(S + B)} \quad (3.22)$$

where

S is the number of signals in the given mass range.

S_0 is the number of signals in the mass range [0, 300 MeV].

B is the number of backgrounds in the given mass range.

\mathcal{E} , P and $\mathcal{E} \times P$ plots as a function of mass width (σ) defined by $\mp k\sigma$ from the peak value where k is the integer from 1 to 5 is shown in Figure 3.22.

* The derivation can be found in Appendix A.

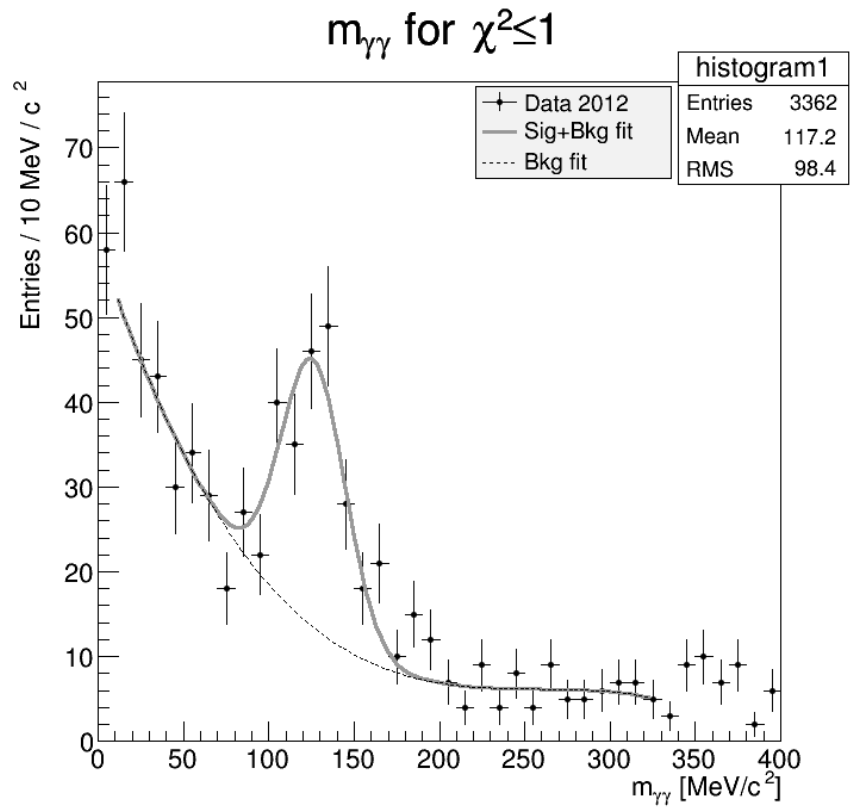


Figure 3.12. Two photon invariant mass distribution for $\chi^2 \leq 1$.

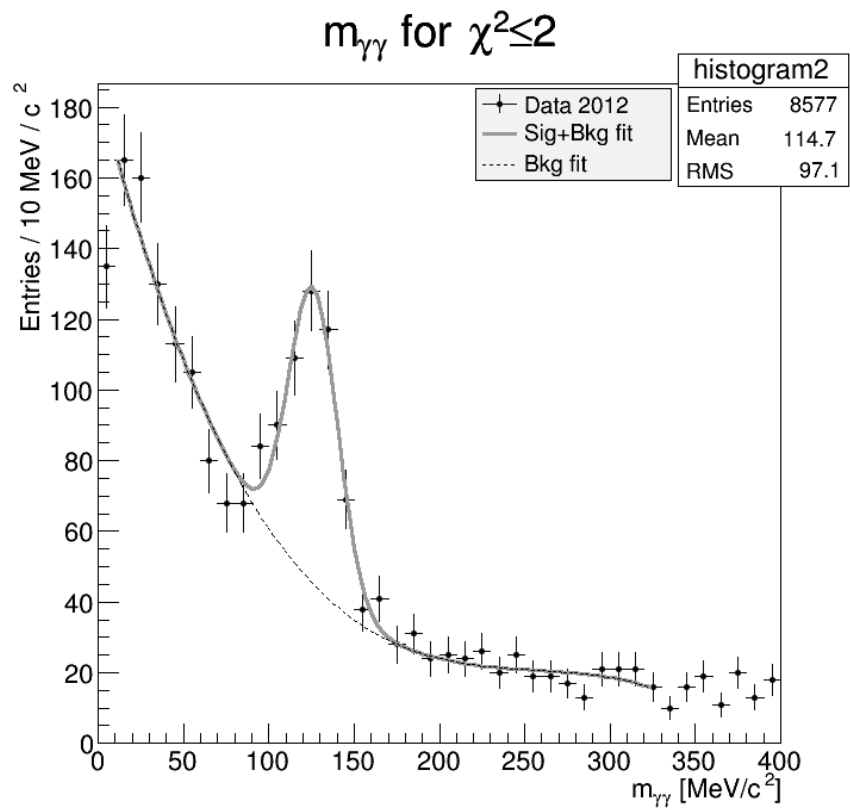


Figure 3.13. Two photon invariant mass distribution for $\chi^2 \leq 2$.

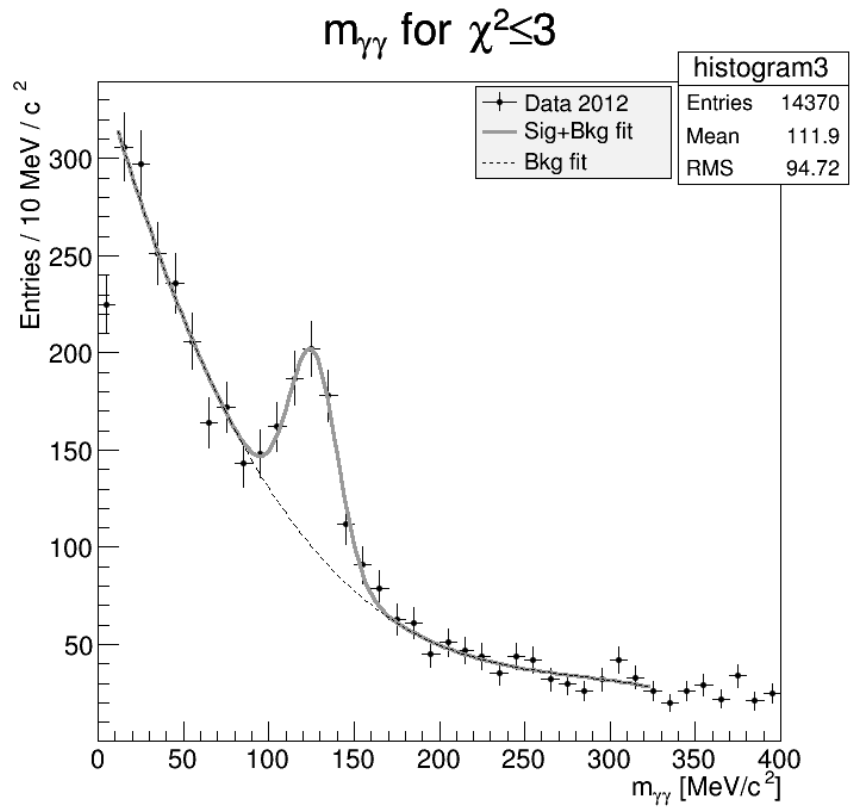


Figure 3.14. Two photon invariant mass distribution for $\chi^2 \leq 3$.

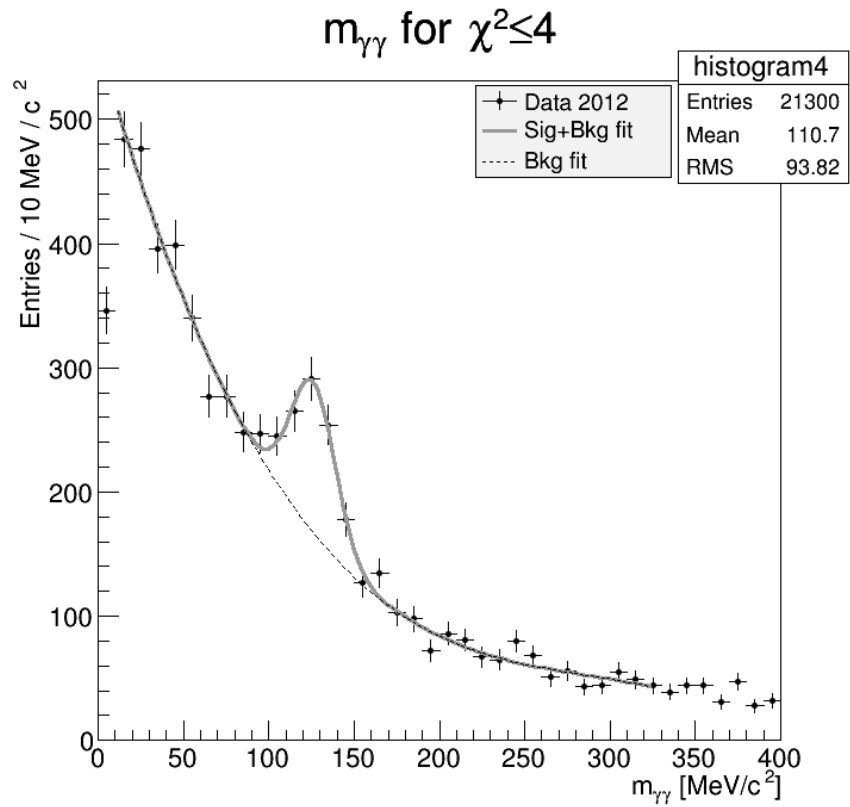


Figure 3.15. Two photon invariant mass distribution for $\chi^2 \leq 4$.

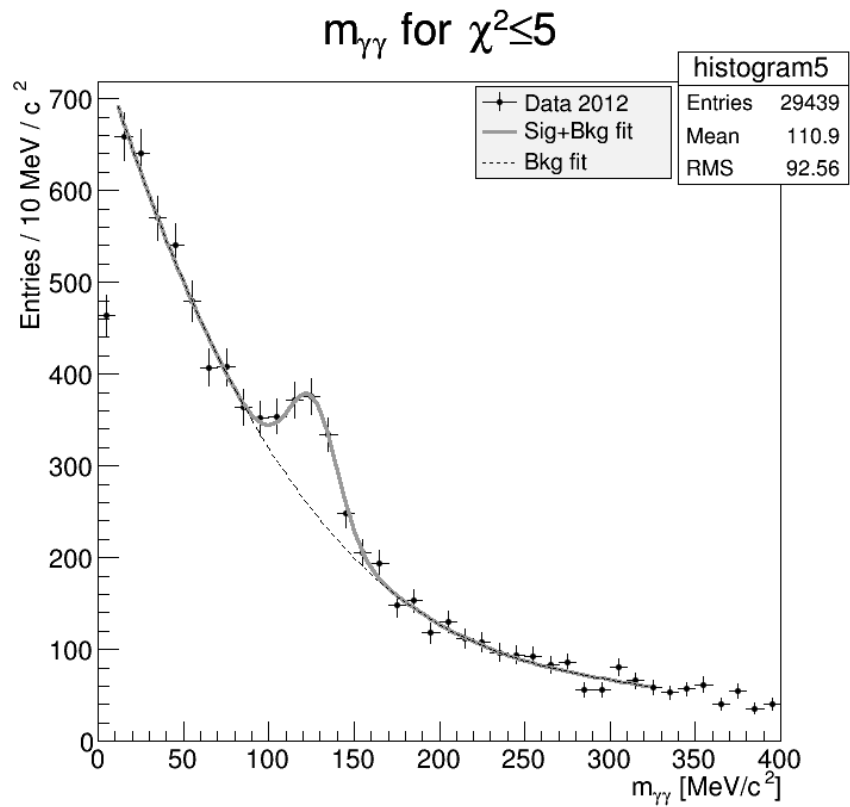


Figure 3.16. Two photon invariant mass distribution for $\chi^2 \leq 5$.

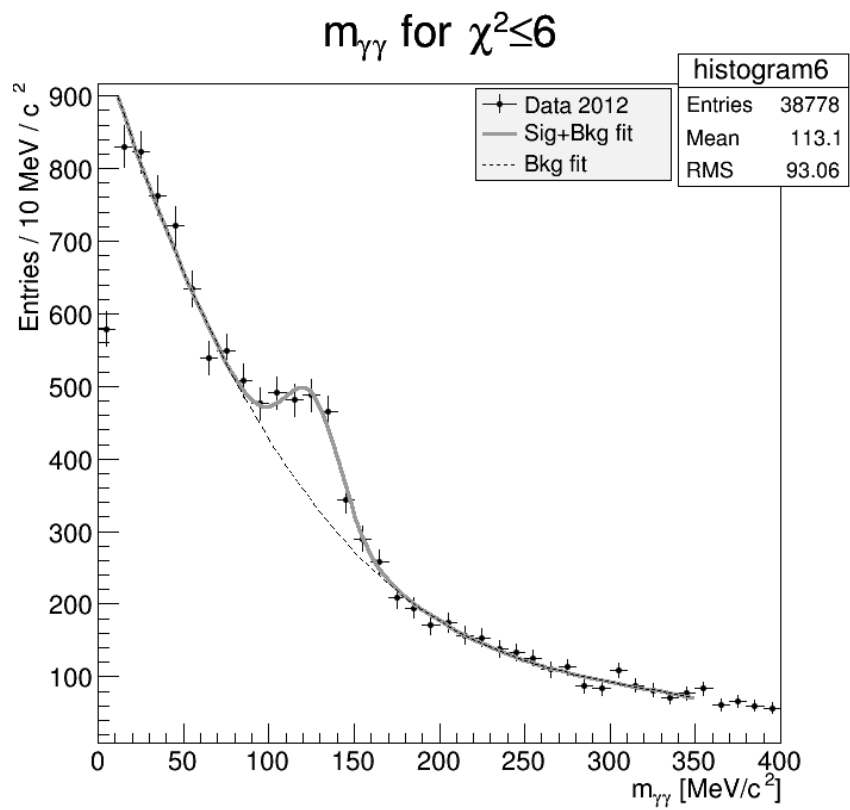


Figure 3.17. Two photon invariant mass distribution for $\chi^2 \leq 6$.

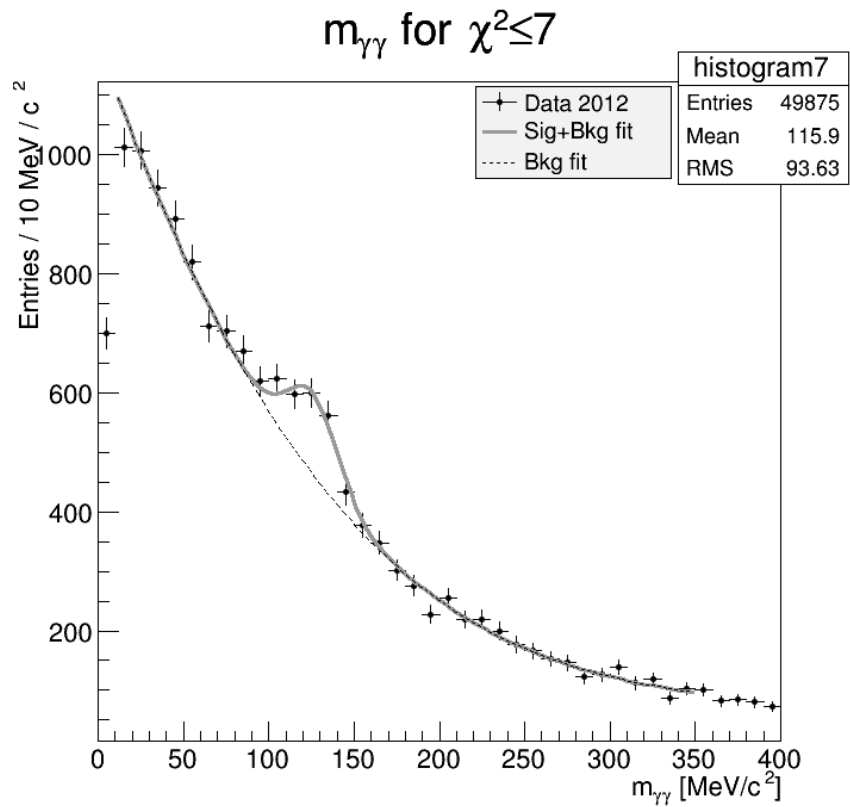


Figure 3.18. Two photon invariant mass distribution for $\chi^2 \leq 7$.

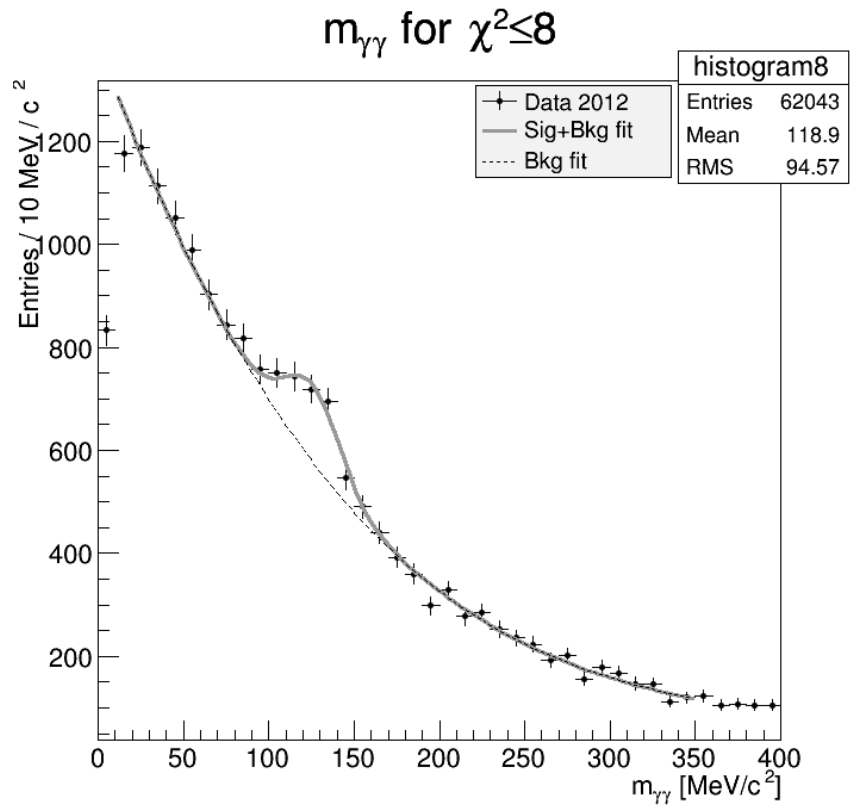


Figure 3.19. Two photon invariant mass distribution for $\chi^2 \leq 8$.

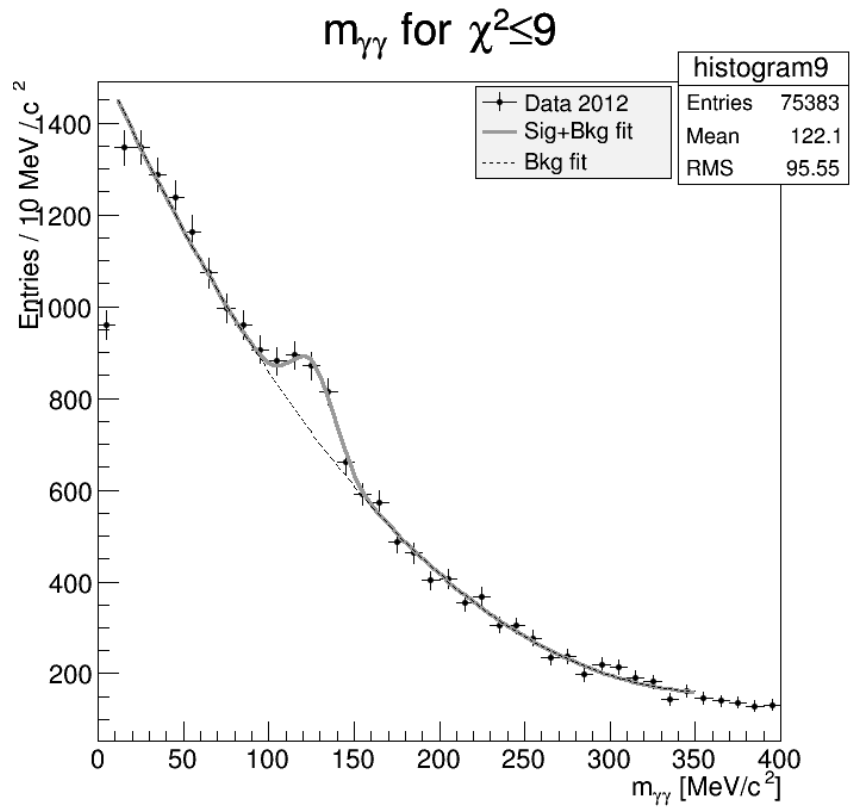


Figure 3.20. Two photon invariant mass distribution for $\chi^2 \leq 9$.

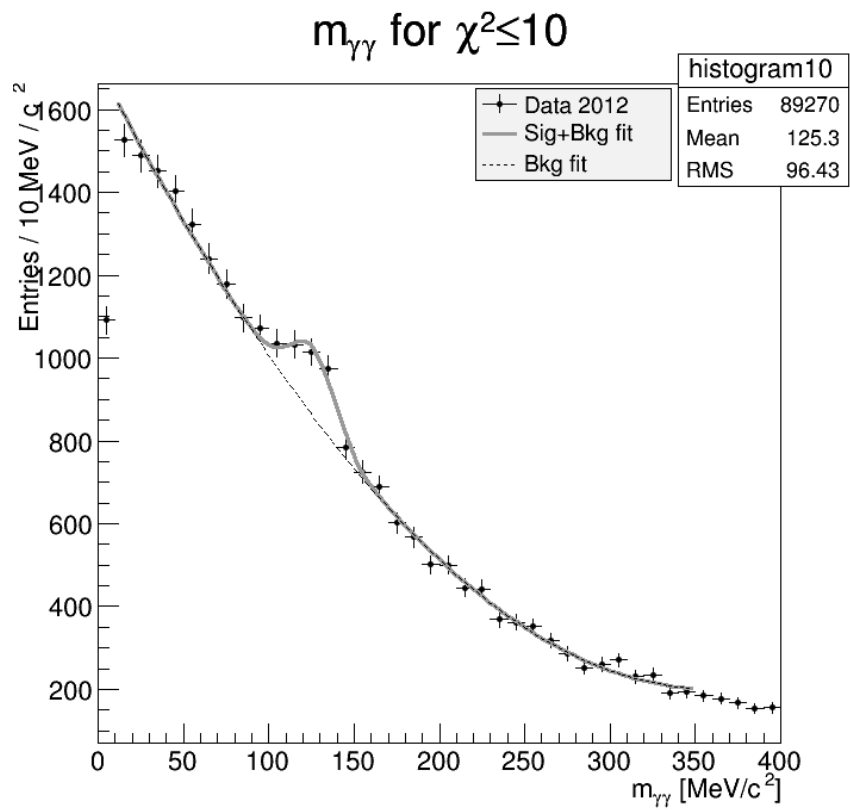


Figure 3.21. Two photon invariant mass distribution for $\chi^2 \leq 10$.

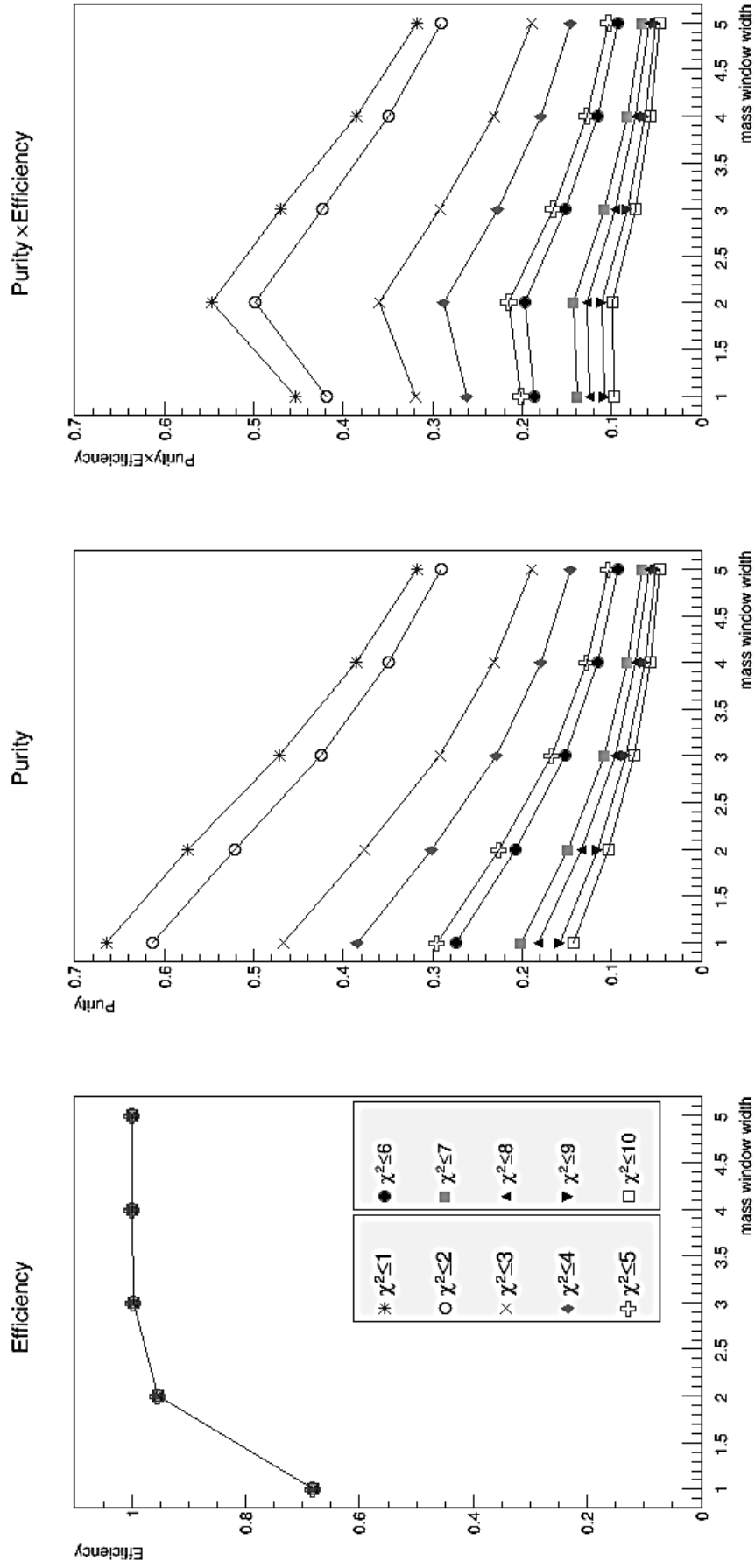


Figure 3.22. Purity, Efficiency and Purity x Efficiency plots as a function of mass width (σ) for different χ^2 values.

Table 3.3: Detailed statistical results for Figure 3.22.

χ^2	σ	S_0	S	B	P	\mathcal{E}	$\mathcal{E} \times P$	S/B
1	1	1492	1018	513	0.6648	0.6826	0.4538	1.9838
	2	1492	1424	1059	0.5735	0.9545	0.5474	1.3448
	3	1492	1488	1668	0.4714	0.9973	0.4701	0.8917
	4	1492	1492	2374	0.3858	0.9999	0.3858	0.6283
	5	1492	1492	3208	0.3174	0.9999	0.3174	0.4650
2	1	3027	2066	1303	0.6132	0.6826	0.4186	1.5854
	2	3027	2889	2650	0.5215	0.9545	0.4978	1.0901
	3	3027	3018	4084	0.4250	0.9973	0.4238	0.7392
	4	3027	3026	5647	0.3489	0.9999	0.3489	0.5359
	5	3027	3027	7385	0.2907	0.9999	0.2907	0.4098
3	1	3614	2467	2823	0.4664	0.6826	0.3184	0.8741
	2	3614	3450	5712	0.3765	0.9545	0.3594	0.6039
	3	3614	3605	8736	0.2921	0.9973	0.2913	0.4126
	4	3614	3614	11960	0.2320	0.9999	0.2320	0.3022
	5	3614	3614	15452	0.1895	0.9999	0.1895	0.2339
4	1	3988	2723	4383	0.3832	0.6826	0.2616	0.6212
	2	3988	3807	8846	0.3008	0.9545	0.2871	0.4303
	3	3988	3978	13471	0.2279	0.9973	0.2273	0.2952
	4	3988	3988	18338	0.1786	0.9999	0.1786	0.2174
	5	3988	3988	23528	0.1449	0.9999	0.1449	0.1695
5	1	4446	3035	7240	0.2954	0.6826	0.2016	0.4192
	2	4446	4244	14610	0.2251	0.9545	0.2148	0.2905
	3	4446	4434	22239	0.1662	0.9973	0.1658	0.1994
	4	4446	4446	30256	0.1281	0.9999	0.1281	0.1469
	5	4446	4446	38791	0.1028	0.9999	0.1028	0.1146
6	1	6207	4237	11232	0.2739	0.6826	0.1870	0.3772
	2	6207	5925	22705	0.2069	0.9545	0.1975	0.2609
	3	6207	6190	34658	0.1515	0.9973	0.1511	0.1786
	4	6207	6207	47332	0.1159	0.9999	0.1159	0.1311
	5	6207	6207	60966	0.0924	0.9999	0.0924	0.1018

7	1	5155	3519	13944	0.2015	0.6826	0.1375	0.2523
	2	5155	4920	28075	0.1491	0.9545	0.1423	0.1752
	3	5155	5141	42575	0.1077	0.9973	0.1074	0.1207
	4	5155	5155	57631	0.0821	0.9999	0.0821	0.0894
	5	5155	5155	73428	0.0656	0.9999	0.0656	0.0702
8	1	6149	4197	18859	0.1820	0.6826	0.1242	0.2225
	2	6149	5869	37968	0.1338	0.9545	0.1277	0.1545
	3	6149	6132	57575	0.0962	0.9973	0.0960	0.1065
	4	6149	6148	77929	0.0731	0.9999	0.0731	0.0789
	5	6149	6149	99279	0.0583	0.9999	0.0583	0.0619
9	1	5043	3443	18368	0.1578	0.6826	0.1077	0.1874
	2	5043	4813	36834	0.1155	0.9545	0.1103	0.1306
	3	5043	5029	55495	0.0831	0.9973	0.0828	0.0906
	4	5043	5043	74451	0.0634	0.9999	0.0634	0.0677
	5	5043	5043	93798	0.0510	0.9999	0.0510	0.0537
10	1	5494	3750	22664	0.1419	0.6826	0.0969	0.1654
	2	5494	5244	45424	0.1035	0.9545	0.0987	0.1154
	3	5494	5479	68376	0.0741	0.9973	0.0739	0.0801
	4	5494	5493	91617	0.0565	0.9999	0.0565	0.0599
	5	5494	5494	115242	0.0455	0.9999	0.0455	0.0476

CHAPTER 4

CONCLUSION

ATLAS is the largest particle detector constructed at LHC to measure a broad spectrum of momenta and energies of particles. Even though ATLAS is designed to reconstruct highly massive and energetic particles, it also allows us to reconstruct light particles.

In this study, the low energetic photon conversion process in ATLAS has been discussed. The conversion candidates are selected from minimum bias events at $\sqrt{s} = 8$ TeV. The Monte Carlo data is used to find differences between signals (conversions) and backgrounds. Some parameters of signals are compared with backgrounds, and some cuts (χ^2 , invariant mass, etc.) are found to eliminate backgrounds. Then these cuts are applied to the real data. Photons are reconstructed from e^+e^- pairs, and then these photons are used to reconstruct π^0 particles built from two-photon invariant mass distribution. A π^0 signal is obtained and fitted with Gaussian function together with a background third-order polynomial function. The purity and efficiency are defined for distributions. The results reveal that the purity of the π^0 signal depends strongly on the χ^2 value of the e^+e^- pairs. Also when we take the $\varepsilon \times P$ value into account, the optimal mass window cut for selecting π^0 candidates is found to be $\pm 2\sigma$ around the π^0 peak.

The same procedure can be applied to $\eta \rightarrow \gamma\gamma$ decays. However this study requires more statistics.

REFERENCES

- [1] CERN Communication Group. (2008). The Large Hadron Collider. Available at: <http://home.web.cern.ch/about/accelerators/large-hadron-collider>. Accessed 13.01.2014.
- [2] The ATLAS Collaboration et al. (2008). The ATLAS Experiment at the CERN Large Hadron Collider. (2008). *JINST* **3** S08003, 1-107.
- [3] LHC Study Group. (1995). The Large Hadron Collider Conceptual Design, *CERN Desktop Publishing Service*, 3-6.
- [4] S.Agostinelli et al. (2003). GEANT4-a simulation toolkit, *Nucl. Instr. Meth. A* 506 250-303.
- [5] T. Sjöstrand, S. Mrenna and P. Skands. (2008). A Brief Introduction to PYTHIA 8.1, *Comput. Phys. Comm.* 178 (2008) 852.
- [6] The ATLAS Collaboration. (2008). Csc note - Photon Conversions in ATLAS. Available at: <http://www.physics.smu.edu/web/research/preprints/SMU-HEP-08-13.pdf>
- [7] Mukund Gupta. (2010). Calculation of radiation of length in materials, PH-EP-Tech-Note-2010-013.
- [8] D.H. Wright et al. (GEANT4 Collaboration). (2012). Physics Reference Manual, 28-33 p.
- [9] J.H.Hubbell, H.A.Gimm, I.Overbo. (1980). Pair, Triplet and Total Atomic Cross Sections (and Mass Attenuation Coefficients) for 1 MeV-100 GeV Photons in Elements Z=1 to 100. *Jou. Phys. Chem. Ref. Data* 9:1023
- [10] J.Beringer et al. (Particle Data Group). (2012). π^0 . *Phys. Rev. D* 86, 10001 (<http://pdg.lbl.gov>)
- [11] A.Bingül. (2007). Inclusive Production of the $\rho^\pm(770)$ Meson in Hadronic Decays of the Z^0 Boson, 65-88 p.

APPENDIX A

π^0 FORMULAE

A.1 Two-Photon Invariant Mass Formula

Consider the decay process of the neutral pion, $\pi^0 \rightarrow \gamma_1 + \gamma_2$. Using natural units, the invariant mass of the photon pairs can be calculated from:

$$\begin{aligned}
 M^2 &= E^2 + p^2 \\
 &= (E_1 + E_2)^2 - (\vec{p}_1 + \vec{p}_2)^2 \\
 &= (E_1 + E_2)^2 - (p_{x_1} + p_{x_2})^2 - (p_{y_1} + p_{y_2})^2 - (p_{z_1} + p_{z_2})^2
 \end{aligned} \tag{A.1}$$

where E_1 and E_2 are the energies of photons that can be found by:

$$E_i^2 = p_i^2 + m_e^2 \tag{A.2}$$

Here $i = 1, 2$ and $p_i^2 = p_{x_i}^2 + p_{y_i}^2 + p_{z_i}^2$. $p_{x,y,z}$ is the momentum components of sum of the photons. m_γ is assumed to be the mass of the photon, thus $m_\gamma = 0$. For the π^0 we can perform reconstruction from two photons. From the conservation of momentum:

$$\vec{p}_{\pi^0} = \vec{p} = \vec{p}_1 = \vec{p}_2 \tag{A.3}$$

Now we can find p^2 via A.3 and definition of dot product of two vectors:

$$\vec{p} \cdot \vec{p} = p^2 = p_1^2 + p_2^2 + 2p_1p_2 \cos \theta_{12} \tag{A.4}$$

where θ_{12} is the angle between two photons. γ_1 and γ_2 are assigned to zero mass, so $E = p$. Thus Equation A.4 becomes:

$$p^2 = E_1^2 + E_2^2 + 2E_1E_2 \cos \theta_{12} \tag{A.5}$$

If we substitute the final result of p^2 into Equation A.1, then:

$$M^2 = 2E_1E_2(1 - \cos \theta_{12}) \tag{A.6}$$

We obtain measurements of E_1 , E_2 and θ_{12} from the electromagnetic calorimeter.

A.2 π^0 Mass Resolution Formula

Mass resolution formula can be derived directly from the invariant mass relation. Equation A.6 can be re-arranged as follows:

$$M = \sqrt{2E_1E_2(1 - \cos \theta_{12})} \quad (\text{A.7})$$

If we assume that E_1 , E_2 and θ_{12} are independent variables, then statistically the mass resolution σ_M can be found from:

$$\begin{aligned} \sigma_M &= \frac{\partial M}{\partial E_1} \sigma_{E_1} \oplus \frac{\partial M}{\partial E_2} \sigma_{E_2} \oplus \frac{\partial M}{\partial \theta_{12}} \sigma_{\theta_{12}} \\ &= \sqrt{\left(\frac{\partial M}{\partial E_1}\right)^2 \sigma_{E_1}^2 + \left(\frac{\partial M}{\partial E_2}\right)^2 \sigma_{E_2}^2 + \left(\frac{\partial M}{\partial \theta_{12}}\right)^2 \sigma_{\theta_{12}}^2} \end{aligned} \quad (\text{A.8})$$

where the square of partial derivatives are:

$$\begin{aligned} \left(\frac{\partial M}{\partial E_1}\right)^2 &= \left(\frac{2E_2(1 - \cos \theta_{12})}{2\sqrt{2E_1E_2(1 - \cos \theta_{12})}}\right)^2 = \frac{E_2(1 - \cos \theta_{12})}{2E_1} \\ \left(\frac{\partial M}{\partial E_2}\right)^2 &= \left(\frac{2E_1(1 - \cos \theta_{12})}{2\sqrt{2E_1E_2(1 - \cos \theta_{12})}}\right)^2 = \frac{E_1(1 - \cos \theta_{12})}{2E_2} \\ \left(\frac{\partial M}{\partial \theta_{12}}\right)^2 &= \left(\frac{2E_1E_2 \sin \theta_{12}}{2\sqrt{2E_1E_2(1 - \cos \theta_{12})}}\right)^2 = \frac{E_1E_2 \sin^2 \theta_{12}}{2(1 - \cos \theta_{12})} \end{aligned} \quad (\text{A.9})$$

One can set up the ratio σ_M/M , after substituting Equations A.9 into A.8.

$$\begin{aligned} \frac{\sigma_M}{M} &= \sqrt{\frac{\sigma_{E_1}^2}{4E_1^2} + \frac{\sigma_{E_2}^2}{4E_2^2} + \frac{\sigma_{\theta_{12}}^2}{4} \frac{\sin^2 \theta_{12}}{(1 - \cos \theta_{12})^2}} \\ &= \frac{1}{2} \sqrt{\frac{\sigma_{E_1}^2}{E_1^2} + \frac{\sigma_{E_2}^2}{E_2^2} + \frac{\sigma_{\theta_{12}}^2}{\tan^2(\theta_{12}/2)}} \\ &= \frac{1}{2} \left[\frac{\sigma_{E_1}}{E_1} \oplus \frac{\sigma_{E_2}}{E_2} \oplus \frac{\sigma_{\theta_{12}}}{\tan(\theta_{12}/2)} \right] \end{aligned} \quad (\text{A.10})$$

The trigonometric expression in Equation A.10 can be transformed as follows:

$$\frac{\sin^2 \theta_{12}}{(1 - \cos \theta_{12})^2} = \frac{1 - \cos^2 \theta_{12}}{(1 - \cos \theta_{12})^2} = \frac{(1 - \cos \theta_{12})(1 + \cos \theta_{12})}{(1 - \cos \theta_{12})(1 - \cos \theta_{12})} = \frac{1 + \cos \theta_{12}}{1 - \cos \theta_{12}}$$

Using half-angle formula, $\cos \beta = \cos^2(\beta/2) - \sin^2(\beta/2)$, we can write:

$$\frac{1 + \cos \theta_{12}}{1 - \cos \theta_{12}} = \frac{1 + \cos^2(\theta_{12}/2) - \sin^2(\theta_{12}/2)}{1 - \cos^2(\theta_{12}/2) + \sin^2(\theta_{12}/2)} = \frac{\cos^2(\theta_{12}/2)}{\sin^2(\theta_{12}/2)} = \frac{1}{\tan^2(\theta_{12}/2)}$$

Hence:

$$\frac{\sin^2 \theta_{12}}{(1 - \cos \theta_{12})^2} = \frac{1}{\tan^2(\theta_{12}/2)}$$